J Mater Sci (2006) 41:6181–6184
DOI 10.1007/s10853-006-0176-7

LETTER

Relations between the creep-rupture properties and the fractal dimension of three-dimensional fracture surface in a cobalt-base alloy

M. Tanaka · Y. Kimura · N. Oyama · R. Kato

Received: 2 August 2005 / Accepted: 28 October 2005 / Published online: 5 August 2006

B.B. Mandelbrot et al. [1] first described the geometrical features of impact fracture surfaces in steels by the fractal dimension, and found that the absorbed energy decreased with increasing fractal dimension of the fracture surface. The fractal dimension of the fracture surface represents self-similarity and complex nature of microstructures on fracture surfaces of materials, depending on the length scale range of the fractal analysis [2]. In the grain-boundary fracture of heat-resistant alloys, the fractal dimension of the fracture surface is associated with steps and ledges, which constitute the grain-boundary serration and are represented by the fractal dimension of the grain boundary, D_{GB} ($1 < D_{GB} < 2$), in the length scale range smaller than one grain-boundary length [3, 4]. The fractal dimension of the fracture surface is also associated with the pattern of grain-boundary microcracks linked to the fracture surface in the length scale range larger than one grain-boundary length [5, 6].

The fractal dimension of the three-dimensional fracture surface can also be deduced from the results of the fractal analysis obtained by the two-dimensional method described above. However, the specimens are considerably damaged by sectioning and polishing during preparation in the two-dimensional method. Computer-aided stereo matching method, which is a non-destructive method, has been successfully applied to the reconstruction of three-dimensional images of fracture surfaces in materials [7–11]. It is desirable to estimate directly the three-dimensional fractal dimension of the fracture surface by the non-destructive method, but it is still unknown whether this method is applicable to severely oxidized fracture surfaces. Therefore, this is an urgent problem to be solved for wide application of the non-destructive three-dimensional fractal analysis to various kinds of fracture surfaces of materials. In this study, the three-dimensional fractal analysis was made on the same specimens of the HS-21 alloy (with various fractal dimensions of the grain boundary, D_{GB}, and the same grain size of 130 μm) as those tested and analysed in the previous study [4, 6], because the results of the three-dimensional method can be compared with those of the two-dimensional method.

Three-dimensional image reconstruction was carried out using stereo pairs of scanning electron micrographs (basic image and tilted image (tilted by 10°)) of fracture surfaces by the computer program of the stereo matching method [11]. Figure 1 shows representative fracture surfaces in the specimens of the HS-21 alloy used for the fractal analysis. More surface cracks and more complicated fracture surface patterns are observed in the specimen with the larger D_{GB} value (Fig. 1b) than in the specimen with the smaller D_{GB} value (Fig. 1a), although the details of grain-boundary microstructures cannot be known because of severe oxidation (Fig. 1e, f). The analysed area is enclosed by a white line in Fig. 1a, b (basic images). The height data

M. Tanaka (✉) · R. Kato
Research Institute of Materials and Resources, Department of Mechanical Engineering, Faculty of Engineering and Resource Science, Akita University, 1-1 Tegatagakuen-cho, Akita 010-8502, Japan
Email: tanaka@mech.akita-u.ac.jp

Y. Kimura
Nippon System Ware Company, 31-11, Sakuragaoka-cho, Shibuya-kuTokyo 150-8577, Japan

N. Oyama
Student of Graduate School, Department of Mechanical Engineering, Faculty of Engineering and Resource Science, Akita University, 1-1 Tegatagakuen-cho, Akita 010-8502, Japan

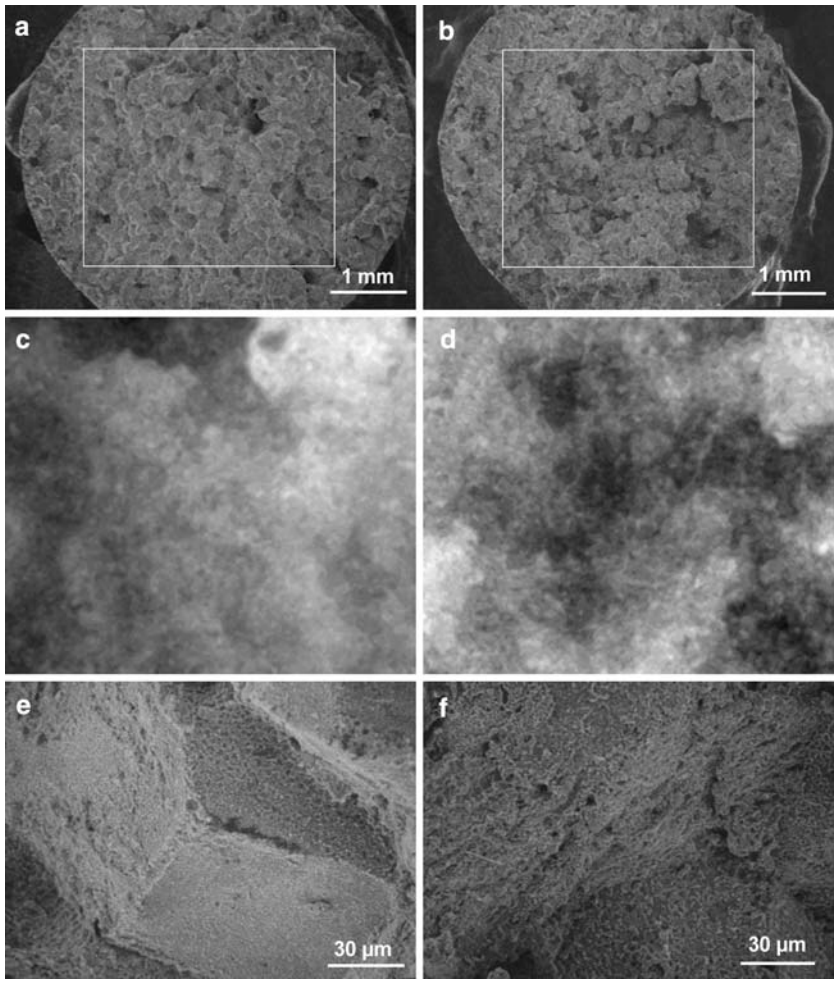

Fig. 1 Representative fracture surfaces in the specimens of the HS-21 alloy used for the fractal analysis. a, c and e are specimen with D_{GB} = 1.056; b, d and f are specimen with D_{GB} = 1.241; a, b, e and f are scanning electron micrographs (the analysed area, 779 × 675 in pixel, is enclosed by white line in a and b); c and d are elevation maps (D_{GB}: fractal dimension of the grain boundary)

(z-direction) of a fracture surface were obtained from the reconstructed three-dimensional image, and were displayed by the color number (from 0 to 255) as an elevation map (a height image) (Fig. 1c, d), while the distance data were given in pixel in the two perpendicular directions (in the x–y plane). The height on the fracture surface increases with increasing color number (brightness) in the height image.

The three-dimensional fractal analysis was made using the elevation maps by the computer program of the box-counting method [12, 13]. In the computer program, three-dimensional fracture surfaces are covered with boxes of rectangular parallelepiped shape with the side length r in the x- and y-directions and with the height cr in the z-direction where c is a constant. The scale for the fractal analysis is considered to be $(cr^3)^{1/3}$ in this case. The number of boxes (N) covering the fracture surface can be related to the ''box size'' (r) through the three-dimensional fractal dimension, D_b ($2 < D_b < 3$), by the following power law relationship:

$$N \propto \{(cr^3)^{1/3}\}^{-D_b} \propto r^{-D_b} \quad (1)$$

where $c^{-D_{b/3}}$ is a constant. Equation (1) can also be written as

$$\log N \propto -D_b \log r \quad (2)$$

The fractal dimension, D_b, can be calculated from Equation (2) by the regression analysis using the datum sets of N and r. The fractal dimension was estimated in the scale length (r) range from 2 pixels to a given size in this study.

There are two fractal dimensions of the three-dimensional fracture surface on the grain-boundary fracture surfaces of the HS-21 alloy, depending on the length scale range of the fractal analysis (Fig. 2a). The fractal dimension of the fracture surface (D_b) lies between about 2.19 and 2.24 and does not clearly depend on the fractal dimension of the grain boundary (D_{GB}) when the value of D_b is estimated in the length scale range smaller one

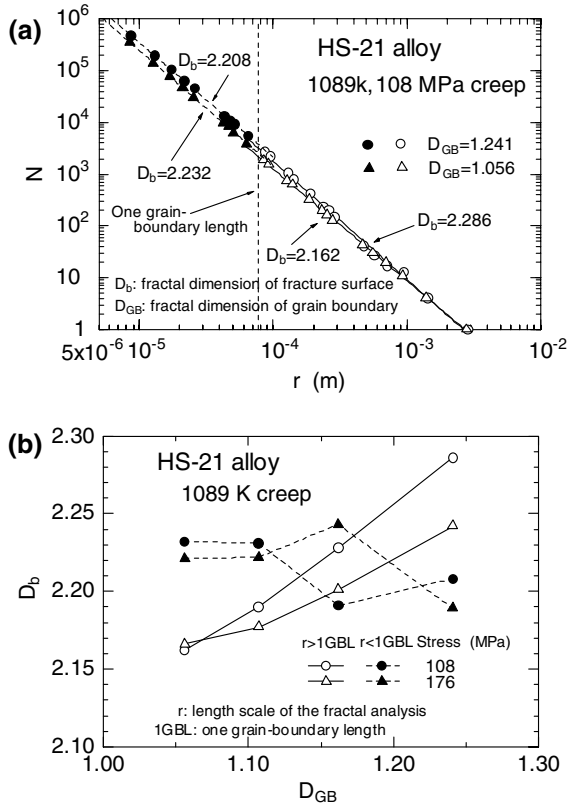

Fig. 2 Fractal dimension of the fracture surface (D_b) and its relation to the fractal dimension of the grain boundary (D_{GB}) in the specimens of the HS-21 alloy ruptured at 973 K. (a) relationship between the number of boxes (N) covering the fracture surface and the box size (r) in the box-counting method (b) relationship between the value of D_b and that of D_{GB}

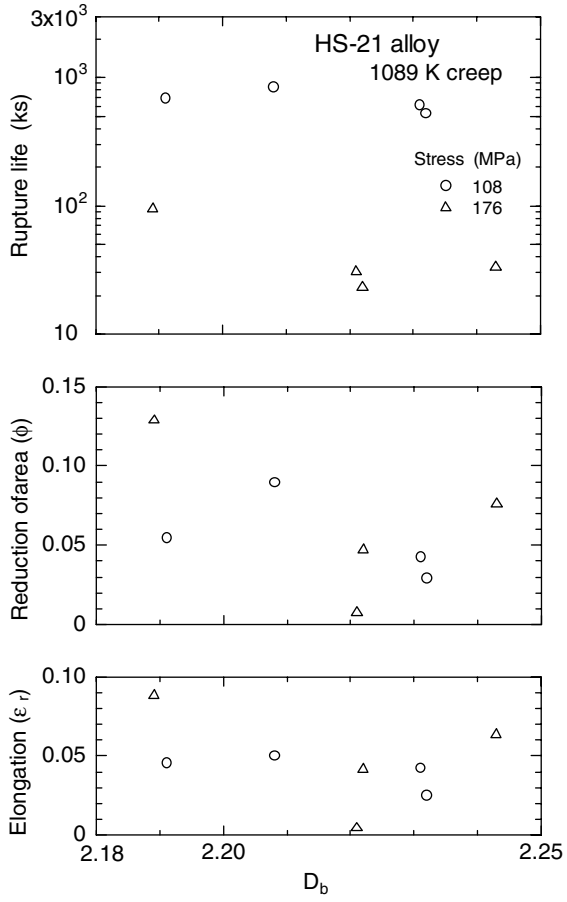

Fig. 3 Relationship between the rupture properties and the fractal dimension of the fracture surface (D_b) estimated in the length scale range smaller than one grain-boundary length in the HS-21 alloy at 973 K

grain-boundary length (about 7.8×10^{-5} m) (Fig. 2b). This result is very different from the results of the two-dimensional fractal analysis, because the fractal dimension of the fracture surface profile estimated in this length scale range is generally larger in the specimens with the larger D_{GB} values [3]. However, when the value of D_b is estimated in the length scale range larger than one grain-boundary length, the value of D_b increases with increasing value of D_{GB}, and is relatively larger under the lower stress (108 MPa) (Fig. 2(b)).

Figure 3 shows the relationship between the creep-rupture properties and the fractal dimension of the fracture surface (D_b) estimated in the length scale range smaller than one grain-boundary length. Both rupture life and creep ductility cannot be correlated with the value of D_b. These results do not coincide with the results of the previous study, because both rupture strength and creep ductility increased with increasing fractal dimension of the fracture surface estimated by the two-dimensional method [3, 4]. In this case, the value of D_b is associated with microstructures like steps or ledges on grain boundaries. However, the oxide layer formed during high-temperature exposure considerably masked the microstructures on grain boundaries (Fig. 1), which were detected by the two-dimensional method [1–3, 5, 6]. This may affect the result of the three-dimensional fractal analysis in the length scale range smaller than one grain-boundary length.

On the contrary, there was no report on the relationship between the rupture properties and the fractal dimension of the three-dimensional fracture surface estimated in the length scale range larger than one grain-boundary length. In this study, both rupture life (t_r) and creep ductility (ϵ_r and ϕ) increase with increasing fractal dimension of the fracture surface (D_b) in the HS-21 alloy when the value of D_b estimated in the length scale range larger than one grain-boundary length (Fig. 4). The relative increase in rupture life or creep ductility with the fractal dimension of the fracture surface (D_b) is larger under the higher stress (176 MPa), although the value of D_b is larger under the lower stress (108 MPa). In polycrystalline materials, the proportion of the amount of grain-boundary sliding to total creep strain generally increases with decreasing stress [14,

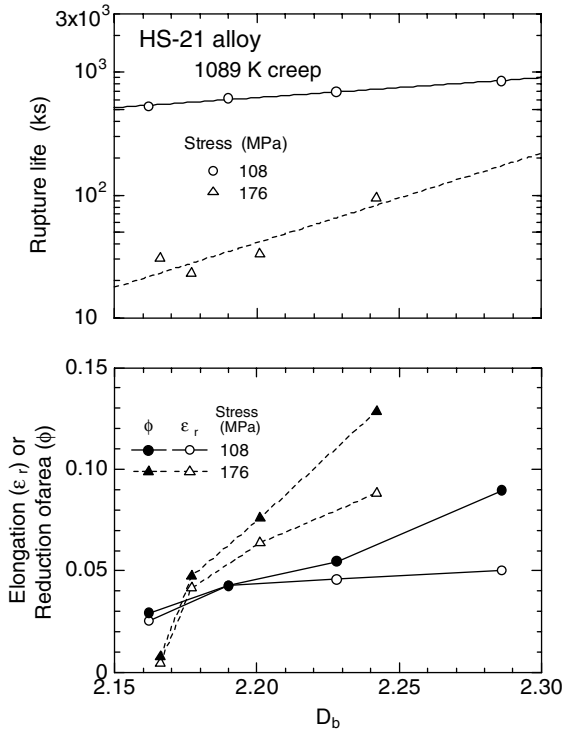

Fig. 4 Relationship between the rupture properties and the fractal dimension of the fracture surface (D_b) estimated in the length scale range larger than one grain-boundary length in the HS-21 alloy at 973 K

15]. Then, more grain-boundary microcracks are formed under the lower stresses, leading to the larger values of the fractal dimension of the fracture surface estimated in the length scale range larger than one grain-boundary length (Fig. 2) [5, 6]. The effect of oxidation on the initiation and growth of the microcracks may be larger at the longer rupture lives. Enhanced grain-boundary sliding and severe oxidation may decrease the toughening effect of serrated grain boundaries under the lower stress (Fig. 4).

Thus, the present fractal analysis using the reconstructed three-dimensional images is also applicable to the fracture surfaces in the specimens of heat-resistant alloys ruptured at high temperature. However, it is necessary to choose carefully the length scale range of the fractal analysis when environmental effects like oxidation of specimen surfaces are not negligible.

Acknowledgements The authors thank The Iron and Steel Institute of Japan (Tekkou-Kenkyu-Shinkou-Josei) for financial support.

References

1. Mandelbrot BB, Passoja DE, Paullay AJ (1984) Nature 308:721
2. Dauskardt RH, Haubensak F, Ritchie RO (1990) Acta Metall 38:142
3. Tanaka M (1992) J Mater Sci 27:4717
4. Tanaka M (1997) J Mater Sci 32:1781
5. Tanaka M (1993) Z Metallkd 84:697
6. Tanaka M (1996) J Mater Sci 31:3513
7. Komai K, Kikuchi J (1985) J Soc Mater Sci Japan 34:648
8. Kobayashi T, Shockey DA (1987) Metall Trans 18A:1941
9. Stampfl J, Scherer S, Berchthaler M, Gruber M, Kolednik O (1996) Int J Fracture 78:35
10. Stampfl J, Kolednik O (2000) Int J Fracture 101:321
11. Tanaka M, Kimura Y, Chouanine L, Taguchi J, Kato R (2003) ISIJ Int 43:1453
12. Mandelbrot BB (1985) The fractal geometry of nature. Translated by H. Hironaka, Nikkei Science, Tokyo
13. Tanaka M, Kimura Y, Chouanine L, Kato R, Taguchi J (2003) J Mater Sci Lett 22:1279
14. Langdon TG, Vastava RB (1982) in ASTM STP 765, American Society for Testing and Materials, Philadelphia, p 435
15. Evans RW, Wilshire B (1985) Creep of metals and alloys. The Institute of Metals, London